Woon Phui Law*, Wan Hanisah Wan Ibrahim and Jolius Gimbun

Modeling of Methyl Methacrylate Polymerization Using MATLAB

DOI 10.1515/cppm-2015-0070
Received December 19, 2015; revised June 3, 2016;
accepted June 5, 2016

Abstract: This paper presents a modeling of methyl methacrylate (MMA) polymerization with toluene in the presence of azo-bi's-isobutyronitrile (AIBN) using MATLAB. This work aims to optimize the initial concentration of initiator and the reactor temperature to achieve a maximum monomer conversion in minimum batch time. The optimization of solution polymerization of MMA based on the three-stage polymerization model (TSPM) was performed using ode23t solver. The non-linear polymerization kinetics considered the gel, glass and cage effect to obtain a realistic prediction. The predicted reactor and jacket temperature showed a reasonable agreement with the experimental data, where the error is about 2.7 % and 2.3 %, respectively. The results showed that a maximum monomer conversion of 94 % was achieved at 0.126 kgmol m^{-3} of the initial concentration of AIBN and 346 K of the initial reactor temperature in 8,951 s (2.5 h).

Keywords: Methyl methacrylate, solution polymerization, ordinary differential equation, optimization, method of moment

1 Introduction

Methyl methacrylate (MMA) is a colorless, volatile organic liquid used for large-scale production of poly-methyl methacrylate (PMMA) via a polymerization process, where the global capacity reached about 0.65 million tons annually [1]. PMMA is widely used for construction, automotive parts, electronic devices and medical applications [2] due to its clarity, light weight and resistance to the effect of UV light and weathering.

According to Lepore et al. [3], bulk polymerization is an exothermic polymerization process. Bulk polymerization often suffers from non-isothermicity due to improper agitation as a result of increasing solution viscosity. Poor mixing affecting the heat dissipation from exothermic polymerization [4] causing a sudden rise in temperature and the gel effect due to decreases in polymer diffusion. The monomer conversion causes an increase in viscosity and hence decreases the initiator diffusion leading to cage effect. Moreover, a sudden rise in temperature and even thermal runaway effect [5] may occur. Temperature plays a significant role in the polymerization kinetics and the polymer properties. As the temperature increases, the molecular weight and viscosity of reactant decrease [6]. As a result, propagation is more likely to occur and hence enhancing the polymerization rate. The glass and cage effect often occurs at temperatures below the glass transition point, whereby the polymer is converted into a glassy state and the movement of the individual chain segments becomes limited. Whereas, the extreme temperature increased the risk of an explosion due to exothermic reactions. Moreover, the reaction rate and the gel effect intensity increase as the temperature reached 423 K or above [7]. The properties of the final product are strongly influenced by the operating condition and the kinetic reactions in the polymerization reactor. Hence, a well-controlled reactor temperature is important to maintain good product quality and for operation safety concern.

The presence of solvent in polymerization process can enhance the reaction stability by reducing the strong gel effect arising from a sudden change in viscosity [7]. Hence, the solvent or solution polymerization like the one in this work is less prone to non-isothermicity issue. Furthermore, the impact of non-isothermicity can be reduced by dilution or cooling to ensure the reactor temperature remains constant. The effect of non-isothermicity in this work has been limited since it is a solvent polymerization performed in a small reactor (3 L) and equipped with a cooling jacket to maintain

***Corresponding author: Woon Phui Law,** Faculty of Chemical & Natural Resources Engineering, Universiti Malaysia Pahang, 26300 Gambang, Pahang, Malaysia, E-mail: woonphui@gmail.com
http://orcid.org/0000-0002-7798-0276
Wan Hanisah Wan Ibrahim, Faculty of Chemical & Natural Resources Engineering, Universiti Malaysia Pahang, 26300 Gambang, Pahang, Malaysia
Jolius Gimbun, Faculty of Chemical & Natural Resources Engineering, Universiti Malaysia Pahang, 26300 Gambang, Pahang, Malaysia; Centre of Excellence for Advanced Research in Fluid Flow, Universiti Malaysia Pahang, 26300 Gambang, Pahang, Malaysia

reactor temperature. It should be noted that bigger reactor is more susceptible to thermal instability than that of small ones. The operation of the solution polymerization reactor is a challenging due to their complex non-linear nature. From economic aspects, high commercial value and maximum yield of polymer in lower possible operating time are the points of interest to be achieved. Hence, this work aims to achieve maximum MMA conversion at a minimum batch time by performing optimization of the operating condition.

The non-linear MMA polymerization kinetic had been studied extensively. Gel and glass effect was modeled according to Chiu et al. [8] and the cage effect was modeled using Achilias and Kiparissides's [9] model. These models have been reported to work well for MMA polymerization [10]. In earlier work, MMA polymerization had been successfully performed using fuzzy-neural model [11], ordinary differential equation solver [12] and Successive Quadratic Programming [13]. Previous works showed that numerical models are useful for optimization and control studies in MMA polymerization operation. In this work, the reactor and jacket dynamics were modeled using MATLAB ode23t. MATLAB is used instead of the experimental technique, because it requires low computational demand besides high-quality data is available for validation and comparison. Ordinary differential equation (ode) is widely used in engineering practice due to many physical laws are couched in terms of the rate of a quantity rather than the magnitude of the quantity itself [14]. Ode solver is divided into two categories, i. e., non-stiff and stiff solvers [15]. The solvers such as ode45, ode23 and ode113 were used for non-stiff problem, whereas ode15s, ode23s, ode23t and ode23tb were used for stiff problem [16]. A stiff system is the one involving rapidly changing components together with the slowly changing ones. In this work, ode23t is employed for the reactor and jacket dynamics modeling. Ode23t is suitable for the moderately stiff problem where the numerical damping is not required in the solution.

The predicted reactor and jacket temperature was compared with the experimental data from Soroush and Kravaris [17]. Once validated, the optimization of concentration of azo-bi's-isobutyronitrile (AIBN) and reactor temperature was performed to achieve a maximum MMA conversion at a minimum batch time. Besides, the effects of the initial concentration of AIBN and reactor temperature on the monomer conversion are also studied.

2 Free radical polymerization kinetic mechanism

It is assumed that solution polymerization follows the standard kinetic scheme, which includes the formation of reactive radicals by the decomposition of AIBN, the reactive addition of monomer units to radical polymer chains in the propagation stage, the growth of a polymer chain is halted in the termination stage and the chain transfer to monomer. The polymerization reaction from MMA to PMMA using AIBN is shown in eq. (1) and the kinetic mechanism of the free-radical polymerization is shown in Table 1 [18–20]. Where I represents initiator, M is monomer, P is live polymer chain, D is dead polymer chain, n, m are monomer units, k_i is the rate coefficient for initiation, k_p is the rate coefficient for propagation, k_{tc} is the rate coefficient for termination by coupling, k_{td} is the rate coefficient for termination by disproportionation and k_{fm} is the rate coefficient for chain transfer to monomer reaction.

$$CH_2C(CH_3)COOCH_3 \underset{AIBN\Delta}{\rightarrow} [CH_2C(CH_3)COOCH_3]_n \quad (1)$$

Table 1: Free radical mechanisms.

Reactions	Mechanisms
Initiation	$I \xrightarrow{k_i} 2\dot{I}$ $\dot{I} + M \xrightarrow{k_{i_0}} P_1$
Propagation	$P_n + M \xrightarrow{k_p} P_{n+1}$
Termination by coupling	$P_n + P_m \xrightarrow{k_{tc}} D_{n+m}$
and disproportionation	$P_n + P_m \xrightarrow{k_{td}} D_n + D_m$
Chain transfer to monomer	$P_n + M \xrightarrow{k_{fm}} D_n + P_1$

3 Polymerization reactor

The polymerization of MMA considered in this work is initiated by AIBN in toluene. AIBN has a good solubility in MMA making them a suitable initiator [21]. In addition, AIBN is safer than other initiators (e. g., benzoyl peroxide) due to its lower explosion risk, besides no oxidation by-products is formed [22] and cause no discoloration, which maintains the physical properties of the polymer [23]. Batch process is often used for MMA polymerization due to its operational flexibility to adjust with the instability of market demand [24].

The pilot-scale batch polymerization reactor considered in this work is similar to the one developed and studied by Soroush and Kravaris [17] at Chemical Process Control Laboratory, The University of Michigan. The MMA polymerization takes place in a 3 L jacketed glass vessel (0.1 m in diameter) equipped with a multi-paddle agitator. The agitator is driven by a constant 250 RPM motor to mix the reacting materials in the reactor. MMA and toluene at the volume ratio of 7:3 were initially added to the process. Then, the mixture was degassed using nitrogen to remove any potential inhibitor (e. g., oxygen). The initiator (AIBN) was introduced once the reactor was heat-up from room temperature to 319.2 K. Soroush and Kravaris [17] measured the temperature of the batch reactor and the jacket system using a resistance temperature detector (RTD). The RTD has a measurement range of 273–373 K with a tolerance of ± 0.2 K. The model developed in this work is compared with the measurement by Soroush and Kravaris [17] for validation purpose, prior to optimization study.

4 Mathematical modeling

The assumptions considered in this work are similar to that of Soroush and Kravaris [17]:

i. All of the reactions are elementary and irreversible.
ii. A perfect mixing is assumed.
iii. Rate of chain transfer to solvent reactions is negligible.
iv. Rate of reaction step is independent of the live polymer chain length.

A polymerization process is affected by the reactor temperature, jacket temperature, initial concentration of initiator, concentration of monomer and dead polymer chains. The energy balance (eqs (2) and (3)) and species balance for initiator, monomer and dead polymer chain (eqs (4)–(8)) are given in the form of ordinary differential equation:

$$\frac{dT}{dt} = \frac{\alpha_o k_p \xi_o C_m}{1+\varepsilon(C_m/C_{mo})} + \alpha_1\left(T_j - T\right) \tag{2}$$

$$\frac{dT_j}{dt} = \alpha_2\left(T - T_j\right) + \alpha_3\left(T_\infty - T_j\right) + \alpha_4\hat{u} \tag{3}$$

$$\frac{dC_i}{dt} = R_i + \varepsilon(C_i/C_{mo})R_m \tag{4}$$

$$\frac{dC_m}{dt} = (1+\varepsilon(C_m/C_{mo}))R_m \tag{5}$$

$$\frac{d\lambda_0}{dt} = \left(1 - Q - \frac{\varepsilon\lambda_0}{C_{mo}}\right)k_p C_m \xi_o \tag{6}$$

$$\frac{d\lambda_1}{dt} = \left(2 - Q - \frac{\varepsilon\lambda_1}{C_{mo}}\right)k_p C_m \xi_o \tag{7}$$

$$\frac{d\lambda_2}{dt} = \left(\frac{4-3Q+Q^2}{1-Q} - \frac{\varepsilon\lambda_2}{C_{mo}}\right)k_p C_m \xi_o \tag{8}$$

where T is reactor temperature, T_j is jacket temperature, C_i is the concentration of initiator, C_m is the concentration of monomer, λ_o, λ_1, λ_2 are the zeroth, first and second moments for the dead polymer chains, respectively. The concentration of live polymer chain and the probability of propagation [5] are given as:

$$\xi_o = (2fk_iC_i/k_t)^{0.5} \tag{9}$$

$$Q = \frac{k_p C_m}{k_p C_m + k_{fm} C_m + k_t \xi_o} \tag{10}$$

where f is the initiator efficiency, k_i, k_p, k_{fm} and k_t are the rate coefficients for initiation, propagation, chain transfer to monomer and termination, respectively. The probability of propagation (Q) is the possibility of an active radical to propagate further instead of terminating and hence Q affects the distribution of polymer chains. A polymer chain formed from an initiation reaction can either undergo propagation or termination. Q is given as the rate of propagation divided by the total of the rates of reactions (R_m, R_{fm}, R_{fs} and R_t) that an active radical may undergo. R_m, R_{fm}, R_{fs} and R_t are given as:

$$R_m = -C_m\xi_o\left(k_p + k_{fm}\right) \tag{11}$$

$$R_{fm} = -C_m\xi_o k_{fm} \tag{12}$$

$$R_{fs} = -C_s\xi_o k_{fs} \tag{13}$$

$$R_t = -\xi_o^2 k_t \tag{14}$$

where the rate of propagation, chain transfer to monomer, chain transfer to solvent and termination are represented by R_m, R_{fm}, R_{fs} and R_t, respectively. The value of k_{fm} is much smaller than k_p, and hence k_{fm} is insignificant in the eq. (11). k_{fs} is ignored since the rate of chain transfer to solvent reaction is negligible in this work. The rate of consumption for initiator is shown as [18, 19]:

$$R_i = -k_iC_i \tag{15}$$

The overall heat transfer rate added to the jacket by the heat transfer fluid is given by:

$$\hat{u} = P - F_{cw}c_w\rho_w\left(T_j - T_{cw}\right) \tag{16}$$

where P is the power input to the heater, F_{cw} and T_{cw} are the inlet flowrate and temperature of cooling water, respectively. c_w and ρ_w are the heat capacity and density of water, respectively. Gel and glass effect models [8] are modeled as:

$$k_p = \frac{k_{po}}{1 + \frac{\xi_o k_{po}}{D k_{\theta p}}} \tag{17}$$

$$k_t = \frac{k_{to}}{1 + \frac{\xi_o k_{to}}{D k_{\theta t}}} \tag{18}$$

where

$$D = \exp\left(\frac{2.3(1-\Phi_p)}{A(T) + B(1-\Phi_p)}\right) \tag{19}$$

$$A = 0.168 - 8.21 \times 10^{-6}(T - T_{gp})^2 \tag{20}$$

$$\Phi_p = \frac{\mu_1/\rho_p}{\frac{\mu_1}{\rho_p} + \frac{C_m M_m}{\rho_m} + \frac{C_s M_s}{\rho_s}} \tag{21}$$

$$\mu_1 = (M_m/(1+\varepsilon))(C_{mo} - C_m) \tag{22}$$

$$C_s = C_{so}\left(\frac{1 + \varepsilon(C_m/C_{mo})}{1+\varepsilon}\right) \tag{23}$$

$$k_{\theta p} = Z_{\theta p} \exp(-E_{\theta p}/RT) \tag{24}$$

$$k_{\theta t} = C_i(0) Z_{\theta t} \exp(-E_{\theta t}/RT) \tag{25}$$

The Arrhenius law for initiation, propagation, termination and chain transfer to monomer are given as:

$$k_i = Z_i \exp(-E_i/RT) \tag{26}$$

$$k_{po} = Z_{po} \exp(-E_{po}/RT) \tag{27}$$

$$k_{to} = Z_{to} \exp(-E_{to}/RT) \tag{28}$$

$$k_{fm} = Z_{fm} \exp(-E_{fm}/RT) \tag{29}$$

The cage effect [9] is modeled as:

$$f = f_o/(1 + (\tau_{DI}/\tau_{RI})) \tag{30}$$

where f and f_o are initiator efficiency at time t and $t = 0$. τ_{DI} and τ_{RI} are the characteristic times corresponded to the radical diffusion and the chain initiation, respectively.

$$\tau_{DI} = r_2^3/3 r_1 D_I \tag{31}$$

$$\tau_{RI} = (k_{io} C_m)^{-1} \tag{32}$$

where

$$r_1 = (6V_m/\pi N_A)^{1/3} \tag{33}$$

$$r_2 = 2r_H \tag{34}$$

$$D_I = D_{Io} \exp\left[-\gamma \hat{V}_I^{\star} M_I \left[(w_m/M_m) + (w_p/M_p)\right]/\hat{V}_f\right] \tag{35}$$

$$\hat{V}_f = w_m \hat{V}_m^{\star} V_{fm} + w_p \hat{V}_p^{\star} V_{fp} \tag{36}$$

$$V_{fm} = 0.149 + 2.9 \times 10^{-4}(T - 273.15) \tag{37}$$

$$V_{fp} = 0.0194 + 1.3 \times 10^{-4}(T - 378.15) \tag{38}$$

$$k_{io} = \in_i k_{po} \tag{39}$$

where r_1 and r_2 are the effective reaction radius at inner and outer diffusion cage, respectively, D_I is a radical diffusion coefficient [25], $\hat{V}_f$ is specific free volume of mixture, V_{fm} and V_{fp} are the free volume of monomer and polymer [26], k_{io} is intrinsic chain initiation rate coefficient and ϵ_i is proportionality coefficient. Theoretically, radical cage is assumed as a sphere [9]. The initial hydrodynamic diameter of the PMMA is computed as:

$$r_H = 1.3 \times 10^{-11} M_w^{0.574} \tag{40}$$

The weight-average molecular weight, number-average molecular weight of dead polymer chain and polydispersity are given by:

$$M_w = M_m(\lambda_2/\lambda_1) \tag{41}$$

$$M_n = M_m(\lambda_1/\lambda_0) \tag{42}$$

$$PDI = M_w/M_n \tag{43}$$

The volume change effect is considered due to the change of density during the conversion of monomer to polymer, the final volume of reacting mixture is given as:

$$V = V_o(1 + \varepsilon x_m) \tag{44}$$

$$\varepsilon = \Phi_{mo}\left(\left(\rho_m/\rho_p\right) - 1\right) \tag{45}$$

$$\Phi_{mo} = C_{mo} M_m/\rho_m \tag{46}$$

where V_o is the initial volume of reacting mixture, ε is volume expansion factor and Φ_{mo} is the initial volume fraction of monomer. A monomer conversion with respect to polymerization time is formulated as:

$$\frac{dx_m}{dt} = -R_m\left(\frac{1+\varepsilon x_m}{C_{mo} + \varepsilon C_m}\right)(1 + \varepsilon(C_m/C_{mo})) \tag{47}$$

All eqs (2)–(47) represent the reactor and jacket dynamics models of the batch MMA polymerization reactor were solved numerically using MATLAB. The model parameters for gel effect, glass effect, cage effect and kinetics are shown in Table 2.

Table 2: Model parameters.

Parameter	Value	Unit	References
B	0.03	–	Baillagou and Soong [18]
C_{so}	8.547	kgmol m^{-3}	Soroush and Kravaris [17]
c	2.2	kJ kg^{-1} K^{-1}	Baillagou and Soong [18]
c_w	4.2	kJ kg^{-1} K^{-1}	Soroush and Kravaris [17]
D_{lo}	2.69×10^{-7}	m^2 s^{-1}	Achilias and Kiparissides [9]
E_{fm}	7.4479×10^{4}	kJ $kgmol^{-1}$	Baillagou and Soong [18]
E_i	1.2877×10^{5}	kJ $kgmol^{-1}$	Baillagou and Soong [18]
E_{po}	1.8283×10^{4}	kJ $kgmol^{-1}$	Baillagou and Soong [18]
E_{to}	2.9442×10^{3}	kJ $kgmol^{-1}$	Baillagou and Soong [18]
$E_{\Theta p}$	1.1700×10^{5}	kJ $kgmol^{-1}$	Baillagou and Soong [18]
$E_{\Theta t}$	1.4584×10^{5}	kJ $kgmol^{-1}$	Baillagou and Soong [18]
F_{cw}	2.0×10^{-6}	m^3 s^{-1}	Soroush and Kravaris [17]
f_o	0.58	–	Tobolsky and Baysal [27]
$(-\Delta H_p)$	5.78×10^{4}	kJ $kgmol^{-1}$	Baillagou and Soong [18]
M_I	68	kg $kgmol^{-1}$	Achilias and Kiparissides [9]
M_m	100.13	kg $kgmol^{-1}$	Achilias and Kiparissides [9]
M_p	150	kg $kgmol^{-1}$	Achilias and Kiparissides [9]
M_s	92.14	kg $kgmol^{-1}$	Baillagou and Soong [18]
m	1.257	kg	Soroush and Kravaris [17]
N_A	6.023×10^{23}	mol^{-1}	–
P	0.55	kJ s^{-1}	Soroush and Kravaris [17]
R	8.345	kJ $kgmol^{-1}$ K^{-1}	–
T_{cw}	279.7	K	Soroush and Kravaris [17]
T_{gp}	387.2	K	Baillagou and Soong [18]
T_{∞}	293.2	K	Soroush and Kravaris [17]
$\hat{V}_I^*$	9.13×10^{-4}	m^3 kg^{-1}	Haward [28]
$\hat{V}_m^*$	8.22×10^{-4}	m^3 kg^{-1}	Haward [28]
V_o	1.5×10^{-3}	m^3	Soroush and Kravaris [17]
$\hat{V}_p^*$	7.7×10^{-4}	m^3 kg^{-1}	Liu et al. [29]
Z_{fm}	4.6610×10^{9}	m^3 $kgmol^{-1}$ s^{-1}	Baillagou and Soong [18]
Z_i	1.0533×10^{15}	s^{-1}	Baillagou and Soong [18]
Z_{po}	4.9167×10^{5}	m^3 $kgmol^{-1}$ s^{-1}	Baillagou and Soong [18]
Z_{to}	9.8000×10^{7}	m^3 $kgmol^{-1}$ s^{-1}	Baillagou and Soong [18]
$Z_{\Theta p}$	3.0233×10^{13}	s^{-1}	Baillagou and Soong [18]
$Z_{\Theta t}$	1.4540×10^{20}	s^{-1}	Baillagou and Soong [18]
α_1	0.0038	s^{-1}	Soroush and Kravaris [17]
α_2	0.0008	s^{-1}	Soroush and Kravaris [17]
α_3	0.00037	s^{-1}	Soroush and Kravaris [17]
α_4	0.0664	K kJ^{-1}	Soroush and Kravaris [17]
ρ_m	915.1	kg m^{-3}	Baillagou and Soong [18]
ρ_s	842	kg m^{-3}	Baillagou and Soong [18]
ρ_p	1,200	kg m^{-3}	Baillagou and Soong [18]
ρ_w	1,000	kg m^{-3}	Soroush and Kravaris [17]
ϵ_i	1	–	Achilias and Kiparissides [9]
Y	0.763	–	Achilias and Kiparissides [30]

5 Formulation of optimization problem

5.1 Reactor temperature

Optimization of reactor temperature (T_o) was performed to obtain a maximum monomer conversion (X_m) in a minimum batch time (t_f^*) using the following algorithm:

$$
\begin{aligned}
&\text{Max} && X_m\\
&\text{Min} && t_f^*\\
&T\\
&\text{s.t.} && f\,(t, X_m(t)) = 0,\ [t_o, t_f] \text{ model equation}\\
& && t_f = 21{,}600\\
& && T_{jo} = 330\\
& && C_{mo} = 6.01\\
& && C_{io} = 0.13\\
& && 295 < T_o < 348
\end{aligned}
$$

The variables, i. e., jacket temperature (T_{jo} = 330 K), initial concentration of monomer (C_{mo} = 6.01 kgmol m^{-3}) and initial concentration of initiator (C_{io} = 0.13 kgmol m^{-3}) were kept constant. Final batch time was set at t_f = 21,600 s.

5.2 Initial concentration of AIBN

An optimization algorithm to obtain a maximum monomer conversion (X_m) in a minimum batch time (t_f^*) by varying the initial concentration of AIBN (C_{io}) was formulated as follows:

Max	X_m
Min	t_f^*
C_{iO}	
s.t.	$f\ (t, X_m(t)) = 0, [t_o, t_f]$ model equation
	t_f = 21,600
	T_{jo} = 330
	C_{mo} = 6.01
	Optimized T_o
	0.05 < C_{io} < 0.14

The variables, i. e., jacket temperature (T_{jo} = 330 K) and initial concentration of monomer (C_{mo} = 6.01 kgmol m^{-3}) were kept constant. Final batch time was set at t_f = 21,600 s.

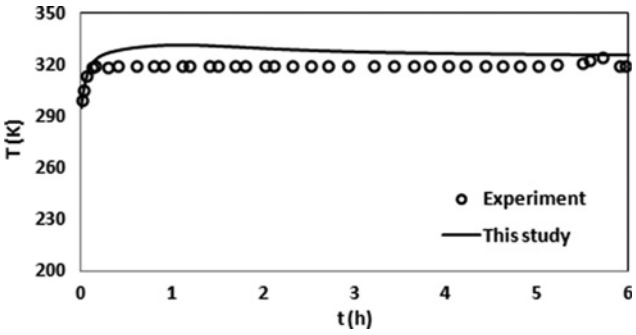

Figure 1: Prediction of the reactor temperature profile against the experimental data adopted from Soroush and Kravaris [17].

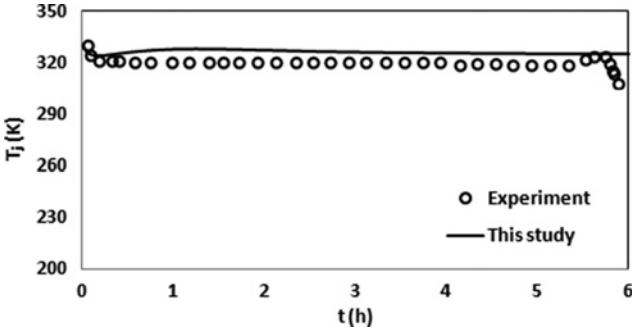

Figure 2: Prediction of the jacket temperature profile against the experimental data adopted from Soroush and Kravaris [17].

6 Results and discussion

6.1 Validation of reactor and jacket temperature

At first, the reactor and jacket dynamic models were solved using ode45 solver, which fails to produce any solution indicating a stiff problem. Thus, a moderately stiff ode23t solver was used to predict the reactor and jacket temperature in the solution polymerization of MMA. The model produced a result within a few seconds. The initial parameters were set at 6.01 kgmol m^{-3} of monomer concentration, 0.13 kgmol m^{-3} of initiator concentration, 295 K of reactor temperature and 330 K of jacket temperature, to enable comparison with Soroush and Kravaris [17]. A final batch time of 21,600 s (6 h) was set for the model.

Figures 1 and 2 show a comparison between the predicted and measured temperature of the reactor and heating/cooling jacket, respectively. Figure 1 shows that the predicted temperature is in good agreement with error about 2.7 % compared to the experimental measurement by Soroush and Kravaris [17]. The model prediction is marginally higher than that experimentally observed which may be attributed by the exclusion of heat loss to surrounding in the model. In the case of a glass jacketed reactor, the heat loss from the reactor is minimal and confined only to the non-jacketed region on the top of the reactor. Solution polymerization of MMA is an exothermic reaction actively releasing excess heat to its surroundings. The predicted jacket temperature profile in Figure 2 also showed marginally higher temperature than the experimental measurement. The deviation between the predicted and measured jacket temperature is about 2.3 %. As shown in Figures 1 and 2, a minor fluctuation was observed experimentally in the reactor and jacket temperature after 5 h of the polymerization process. According to Soroush and Kravaris [17], this fluctuation is caused by the high viscosity of reacting mixture and the coalescence of the nitrogen bubbles. A thick polymer layer was then formed and affecting the overall heat transfer in the batch reactor. The reactor control system triggers a sharp change in the manipulated inputs (power input to the heater, P and coolant flowrate, F_{cw}) to adhere to the set point and hence, resulting in a minor fluctuation. In contrast, a constant heat transfer coefficient and

a perfect mixing were assumed in MATLAB modeling. Thus, no fluctuation of temperature was obtained for the predicted temperature in Figures 1 and 2. This is the reason that the predicted result of this study does not fully match with the experimental temperature measured by Soroush and Kravaris [17], especially after the 5 h of operation. However, a fair agreement was obtained from the predicted temperature throughout the polymerization process with 2.7 % and 2.3 % of deviation from the measured reactor and jacket temperature, respectively. Hence the developed model can be used for optimization study.

6.2 Optimization of initial condition

The initial condition for monomer concentration of 6.01 kgmol m^{-3}, 0.13 kgmol m^{-3} of initiator concentration and 330 K of jacket temperature were set to evaluate the effect of reactor temperature. Table 3 shows the effect of the reactor temperature on conversion of monomer obtained from the optimization study. The result shows that a higher temperature promotes better initiator decomposition and also enhanced the reaction between the initiator and monomer, resulting in a higher conversion of monomer, as shown in Table 3. Temperature strongly affects the initiator decomposition and conversion of MMA. The conversion of MMA increases as the reactor temperature increase from 295 to 345 K. A sufficiently high temperature is important to reduce the diffusion resistance caused by the gel effect. Nevertheless, the conversion of MMA decreases as the temperature increased beyond 345 K. This may be due to the degradation of monomer often associated with high-temperature polymerization. Table 3 shows that MMA conversion over 0.90 was achieved at a temperature ranged from 344 to 346 K. As reactor temperature increases from 344 to 345 K, the MMA conversion increases from 0.91 to 0.95, as well as the batch time. The monomer conversion decreased to 0.92 as the temperature increased to 346 K, but at the same time the batch time dropped dramatically from 21,146 to 7,011 s. Thus, the reactor temperature of 346 K was chosen as the optimum condition which produces conversion of 92 % and residence time of 7,011 s.

The initial condition corresponds to 6.01 kgmol m^{-3} of monomer concentration, 346 K of reactor temperature and 330 K of jacket temperature were used to evaluate the optimum initial concentration of AIBN for the MMA polymerization in this work. Table 4 shows the effect of the initial concentration of AIBN on conversion of monomer obtained from the optimization study. As shown in Table 4, the MMA conversion increases from 0.67 to 0.94 as the initial concentration of AIBN increased from 0.05 to 0.128 kgmol m^{-3}. This is because increasing the concentration of AIBN increased the probability of AIBN to react with MMA, hence enhancing the polymerization process. However, the conversion of MMA decreases as the concentration of AIBN increased beyond 0.128 kgmol m^{-3}, although the batch time is decreasing. Different concentration of AIBN requires a different induction time because the induction duration corresponds to the decomposition of

Table 3: Effect of initial reactor temperature on monomer conversion.

Temperature, T_o (K)	Conversion, X_m	Time, t_f^* (s)
295	0.80	20,842
300	0.81	21,469
310	0.81	20,935
320	0.82	21,064
330	0.83	20,741
340	0.86	20,381
341	0.87	20,728
342	0.88	20,880
343	0.89	20,375
344	0.91	20,150
345	0.95	21,146
346*	**0.92**	**7,011**
347	0.85	2,115
348	0.81	4,368

Note: *Optimum point.

Table 4: Effect of initial concentration of AIBN on monomer conversion.

Concentration, C_{io} (kgmol m^{-3})	Conversion, X_m	Time, t_f^* (s)
0.05	0.67	21,298
0.10	0.84	20,840
0.11	0.88	21,524
0.12	0.92	18,556
0.121	0.92	16,105
0.122	0.93	16,337
0.123	0.93	13,005
0.124	0.94	13,901
0.125	0.94	10,840
0.126*	**0.94**	**8,951**
0.127	0.94	9,636
0.128	0.94	15,108
0.129	0.93	11,745
0.13	0.92	7,011
0.14	0.85	2,101

Note: *Optimum point.

AIBN itself. The optimum initial concentration of AIBN was found at 0.126 kgmol m^{-3} which yielded a maximum conversion of 0.94 at the shortest batch time (8,951 s).

6.3 Effect of AIBN concentration

Conversion of MMA is significantly affected by the initial concentration of AIBN, as shown in Figures 3 and 4. Figure 3 showed a sudden drop of the AIBN concentration from 0.126 to 0.02 kgmol m^{-3}, while the conversion of MMA increased instantly to 0.90 within the first 1,500 s (Figure 4). The instant polymerization reaction is due to the presence of a sufficient amount of AIBN in the reactor and hence promoting the reaction between the decomposed AIBN and MMA, as well as enhancing the propagation rate. After 1,500 s, a sufficiently large amount of long chain polymer occupied most of the reactor volume, hence reducing the probability of AIBN and MMA to react. Furthermore, the amount of the remaining AIBN is limited as the polymerization reaction progresses. Thus, the rate of propagation is limited and the concentration of AIBN shows almost a plateau profile after the first 1,500 s.

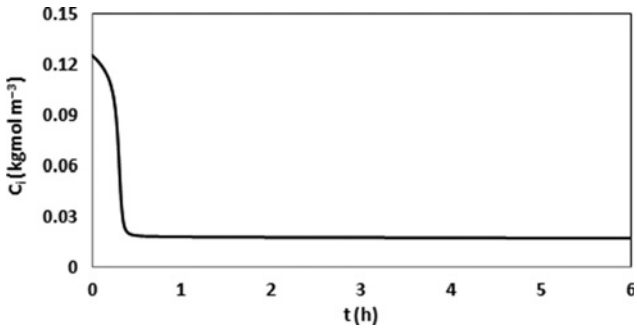

Figure 3: Concentration of AIBN, C_i (kgmol m^{-3}) versus time, t (h).

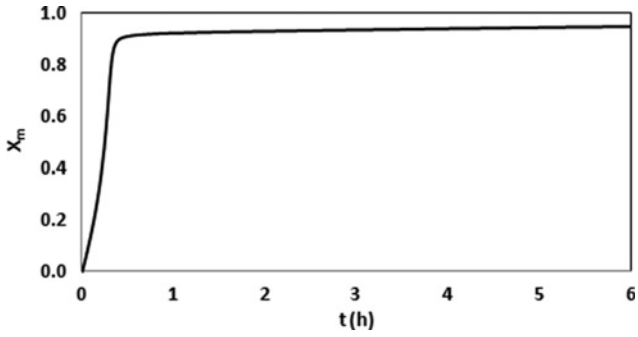

Figure 4: Monomer conversion, X_m versus time, t (h).

6.4 Effect of reactor temperature

Figure 5 shows the reactor temperature profile for the solution polymerization of MMA. Temperature fluctuation was observed in Figure 5, whereby the reactor temperature suddenly increased from 346 K to the maximum of 387.7 K in the first 1,500 s. This is due to a large amount of heat released from the exothermic reaction between MMA and AIBN which corresponds to a large consumption of AIBN and MMA as showed in Figures 3 and 6, respectively. As a result, a maximum conversion of MMA (close to 100 %) was obtained as shown in Figure 4. After 1,500 s, the propagation reaction reduced due to the limited amount of remaining reactants. The reactor temperature stays nearly constant at about 324 K from a time between 2 to 6 h, after the initial temperature spike.

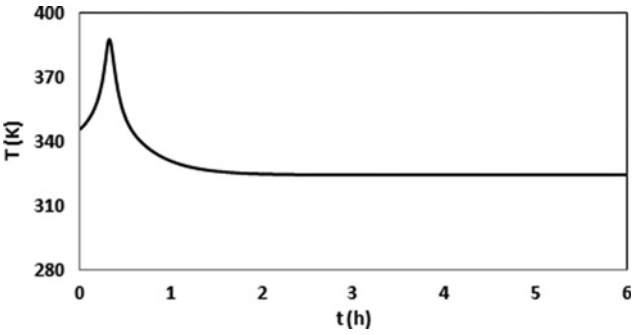

Figure 5: Reactor temperature, T (K) versus time, t (h).

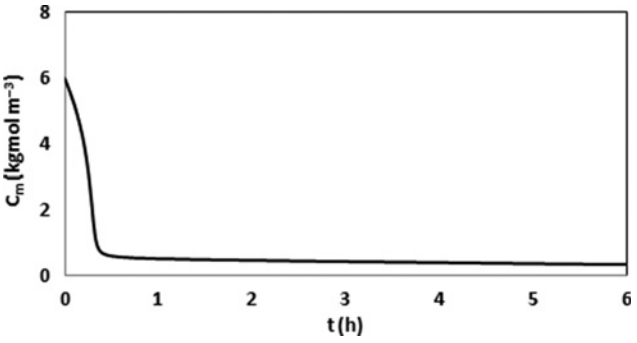

Figure 6: Concentration of MMA, C_m (kgmol m^{-3}) versus time, t (h).

Figure 7 shows the rate coefficients' plot along the polymerization time. A sudden rise of the values for all the rate coefficients in the first 1,500 s was observed, which coincide with the sudden increase in temperature due to a fast polymerization reaction occurring at the same time (see Figures 4 and 5). Higher temperature induced faster movement and higher collision rate between reactants.

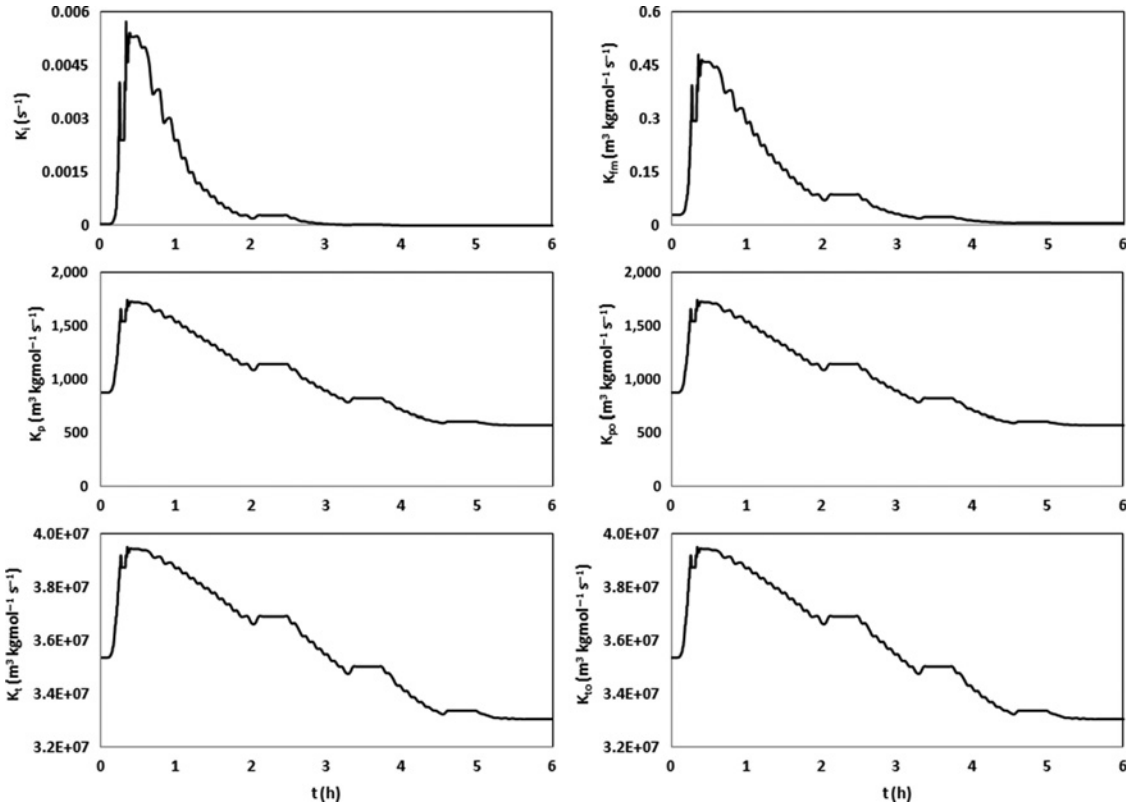

Figure 7: Rate coefficients, k_i, k_p, k_t, k_{fm}, k_{po}, k_{to} versus time, t (h).

Higher collision rate results in a higher kinetic energy, in which the reactants are sufficiently energetic (kinetic energy should be higher than the activation energy) to ensure the reaction to occur. This implies that a faster polymerization reaction is much more likely at a higher reactor temperature for a process with a lower activation energy. The simulation results showed that approximately 4 % increase in the rate coefficients for every 10 K rise in temperature. A smaller rate coefficient values were observed for k_i and k_{fm} due to their larger activation energies (E_i and E_{fm}) compared to others i. e. k_p, k_{po}, k_t and k_{to}. It was also observed that k_i and k_{fm} increased and dropped much faster than the other rate coefficients (k_p, k_{po}, k_t and k_{to}). The rate coefficients steadily dropped after the first 1,500 s as the reactant becomes limited. After 7,200 s, no substantial change was observed in all rate coefficients, as the reactor temperature is kept constant around 324 K. An approximately isothermal condition is maintained after 7,200 s. This work showed that the rate coefficients are strongly affected by their activation energies and the reactor temperature.

Figure 8 shows the zeroth, first and second moments for dead polymer chains. Dead polymer chain is formed during the termination reaction where the polymer chain is

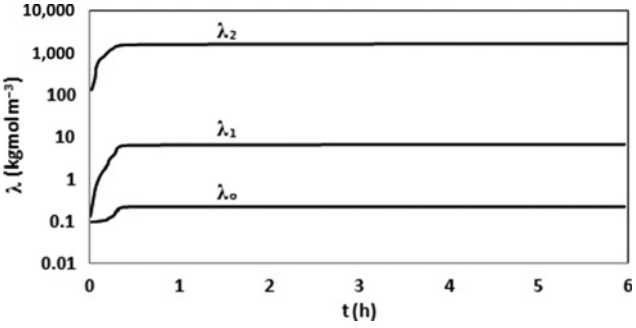

Figure 8: Zeroth, first and second moments for dead polymer chains.

incapable of further growth. Sharp increases in dead polymer chains concentration in the first 1,500 s are caused by the increases of termination rate (k_t in Figure 7). However, the monomer conversion in this work is not affected by the dead polymer chain formation. As shown in eqs (9) and (11), the propagation reaction depends on k_t^a, where the exponent |a| is small (0.5). Therefore, the propagation reaction still occurs, even though k_t is much larger than the k_p as shown in Figure 7.

Figures 9–11 show the weight-average molecular weight (M_w), number-average molecular weight of dead

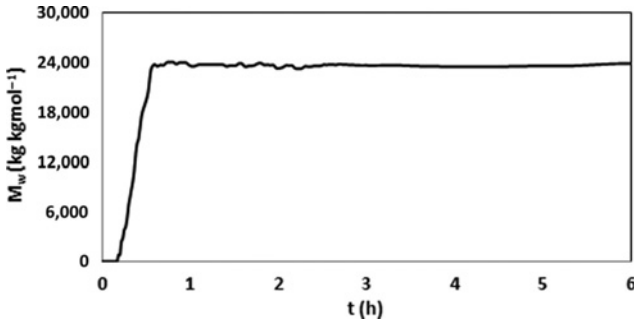

Figure 9: Evolution of weight-average molecular weight, M_w (kg kgmol^{-1}).

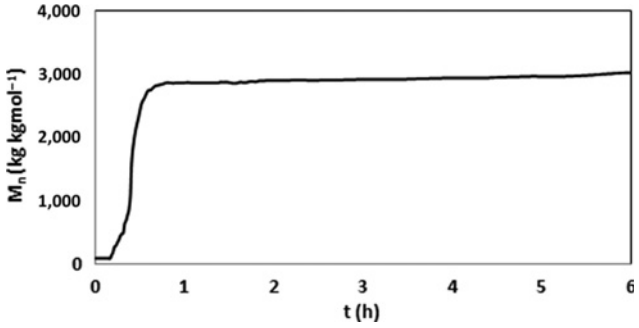

Figure 10: Evolution of number-average molecular weight, M_n (kg kgmol^{-1}).

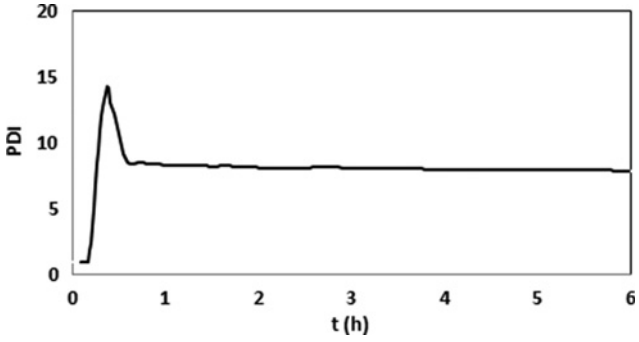

Figure 11: Evolution of polydispersity index (PDI).

polymer chains (M_n) and polydispersity index (PDI), respectively. The evolution of M_w and M_n in Figures 9 and 10 are similar as the monomer conversion in Figure 4 and the moments plot in Figure 8. As monomer conversion increases, the viscosity of reacting mixture increases. This causes a cage effect and the polymer chain stopped growing. In the meantime, the formation of a dead polymer chain is increasing due to the termination of polymerization in the first 1,500 s. Hence, M_w and M_n are increasing as well. PDI is a measure of polymer molecular weight distribution. A polydisperse polymer has a PDI > 1, where all the molecules consist of different chain length. While a monodisperse polymer consists of similar length chains (PDI = 1). Usually, chain polymerization yielded values of PDI between 1.5 and 20. PDI values increase as a reaction product becomes more heterogeneous owing to the difficulty of controlling the operating conditions in exothermic and non-linear polymerization process. In this work, PMMA is polydisperse with the PDI is about 7.9. The physical properties and mechanical properties (e. g., tensile strength, impact resistance and elasticity) of polymers are affected by their molecular weight. The desired polymer products should have a sufficiently long chain length (high M_n) and low PDI.

7 Conclusion

The optimization of solution polymerization of MMA with toluene in the presence of AIBN as the initiator was performed using MATLAB. The model prediction showed good agreement with the experimental data with about 2.7 % and 2.3 % of deviation in the reactor temperature and jacket temperature, respectively. This work indicated that 94 % of MMA conversion at a minimum batch time of 8,951 s (2.5 h) can be achieved using the initial AIBN concentration of 0.126 kgmol m^{-3} and initial reactor temperature of 346 K. The results of this work demonstrated that MATLAB can be employed to perform an optimization study of MMA polymerization effectively and economically.

Nomenclature

A	Temperature dependent coefficient in gel effect model
B	Constant parameter in gel effect constant
C_i	Concentration of initiator, kgmol m^{-3}
C_{io}	Initial concentration of initiator, kgmol m^{-3}
C_m	Concentration of monomer, kgmol m^{-3}
C_{mo}	Initial concentration of monomer, kgmol m^{-3}
C_s	Concentration of solvent, kgmol m^{-3}
C_{so}	Initial concentration of solvent, kgmol m^{-3}
c	Heat capacity of reacting mixture, kJ kg^{-1} K^{-1}
c_w	Heat capacity of water, kJ kg^{-1} K^{-1}
D	Intermediate variable in gel and glass effect models
D_I	Radical diffusion coefficient, m^2 s^{-1}
D_n	Dead polymer chain with n unit of monomers
E_{fm}	Activation energy for chain transfer to monomer, kJ kgmol^{-1}
E_i	Activation energy for initiation, kJ kgmol^{-1}
E_{po}, E_{to}	Activation energy for rate coefficient k_{po} and k_{to}, kJ kgmol^{-1}

$E_{\theta p}$, $E_{\theta t}$ Activation energy for parameter $k_{\theta p}$ and $k_{\theta t}$, kJ kgmol^{-1}
F_{cw} Cooling water flowrate, m^3 s^{-1}
f, f_o Initiator efficiency at time t and $t = 0$
ΔH_p Heat of propagation rate, kJ kgmol^{-1}
I Initiator
k_{fm} Rate coefficient for chain transfer to monomer, m^3 kgmol^{-1} s^{-1}
k_{fs} Rate coefficient for chain transfer to solvent, m^3 kgmol^{-1} s^{-1}
k_i Rate coefficient for initiation, s^{-1}
k_{io} Intrinsic chain initiation rate coefficient, m^3 kgmol^{-1} s^{-1}
k_p Rate coefficient for propagation, m^3 kgmol^{-1} s^{-1}
k_{po}, k_{to} Overall propagation and termination rate coefficient at zero monomer conversion, m^3 kgmol^{-1} s^{-1}
k_{tc}, k_{td} Rate coefficient for termination by combination and disproportionation reactions, m^3 kgmol^{-1} s^{-1}
$k_{\theta p}$ Temperature dependent coefficient in gel effect model
$k_{\theta t}$ Temperature and initiator loading concentration dependent parameter in gel effect model
M Monomer
M_I Molecular weight of initiator, kg kgmol^{-1}
M_m Molecular weight of monomer, kg kgmol^{-1}
M_p Molecular weight of polymer, kg kgmol^{-1}
M_s Molecular weight of solvent, kg kgmol^{-1}
M_w Weight-average molecular weight of dead polymer chain, kg kgmol^{-1}
m Mass of reacting mixture, kg
N_A Avogadro's number, mol^{-1}
P Heater power input, kJ s^{-1}
P_n Live polymer chain consisting of n monomer units
Q Probability of propagation
R Universal gas constant, kJ kgmol^{-1} K^{-1}
R_m, R_i Rate of consumption for monomer and initiator, kgmol m^{-3} s^{-1}
r_H Hydrodynamic diameter of PMMA, m
r_1 Effective radius at inner diffusion cage, m
r_2 Effective radius at outer diffusion cage, m
T Reactor temperature, K
T_{cw} Cooling water temperature, K
T_{gp} Glass transition temperature of PMMA, K
T_j Jacket temperature, K
T_o Initial reactor temperature, K
T_∞ Room temperature, K
t Time, s
t_f Final batch time, s
$\hat{u}$ Overall rate of heat added to jacket, kJ s^{-1}
V Final volume of reacting mixture, m^3
V_{fm} Free volume of monomer
V_{fp} Free volume of polymer
V_m Volume of monomer, m^3
V_o Initial volume of reacting mixture, m^3
$\hat{V}_f$ Specific free volume of reacting mixture, m^3 kg^{-1}
$\hat{V}_I^*$ Critical volume of initiator, m^3 kg^{-1}
$\hat{V}_m^*$ Critical volume of monomer, m^3 kg^{-1}
$\hat{V}_p^*$ Critical volume of polymer, m^3 kg^{-1}
w_m Weight fraction of monomer
w_p Weight fraction of polymer
x_m Monomer conversion
Z_{fm} Frequency factor for chain transfer to monomer, m^3 kgmol^{-1} s^{-1}
Z_i Frequency factor for chain transfer to monomer, s^{-1}
Z_{po} Frequency factor for rate coefficient k_{po}, m^3 kgmol^{-1} s^{-1}
Z_{to} Frequency factor for rate coefficient k_{to}, m^3 kgmol^{-1} s^{-1}
$Z_{\theta p}$ Frequency factor for $k_{\theta p}$, m^3 kgmol^{-1} s^{-1}
$Z_{\theta t}$ Frequency factor for $k_{\theta t}$, m^3 kgmol^{-1} s^{-1}

Symbols

ε Volume expansion factor
α Process parameter
ξ_o Concentration of live polymer chain, kgmol m^{-3}
λ_o, λ_1, λ_2 Zeroth, first and second moments for dead polymer chains, kgmol m^{-3}
ρ_m Density of monomer, kg m^{-3}
ρ_s Density of solvent, kg m^{-3}
ρ_p Density of polymer, kg m^{-3}
ρ_w Density of water, kg m^{-3}
μ_1 Mass concentration of dead polymer chain, kg m^{-3}
Φ_p Volume fraction of polymer
Φ_{mo} Initial volume fraction of monomer
ϵ_i Proportionality coefficient
Y Overlap factor
τ_{Dl}, τ_{Rl} Characteristic times for radical diffusion and chain initiation, s

References

1. Lin J, Mirasol F. PMMA market to get a jolt from the growing electronics sector. ICIS Chemical Business, 2011. Available at: http://www.icis.com. Accessed: 7 Sep 2015.
2. Dormer W, Gomes R, Meek ME. Methyl methacrylate. Concise International Chemical Assessment Document 4. Geneva: World Health Organization, 1998.
3. Lepore R, Vande Wouwer A, Remy M, Findeisen R, Nagy Z, Allgower F. Optimization strategies for a MMA polymerization reactor. Comp Chem Eng 2007;31(4):281–91.
4. Berins ML. SPI Plastics engineering handbook of the society of the plastics industry, Inc., 5th ed. New York: Springer Science and Business Media, 2012.
5. Crowley TJ, Choi KY. On-line monitoring and control of a batch polymerization reactor. J Proc Cont 1996;6(2):119–27.
6. Nising P, Meyer T. Modeling of the high-temperature polymerization of methyl methacrylate. 1. Review of existing models for the description of the gel effect. Ind Eng Chem Res 2004;43 (23):7220–6.
7. Nising P. High temperature radical polymerization of methyl methacrylate in a continuous pilot scale process (PhD thesis). Lausanne: Erlangen-Nurnberg University, 2006.
8. Chiu WY, Carratt GM, Soong DS. A computer model for the gel effect in free-radical polymerization. Macromolecules 1983; 16(3):348–57.
9. Achilias DS, Kiparissides C. Development of a general mathematical framework for modelling diffusion-controlled free-radical polymerization reactions. Macromolecules 1992;25 (14):3739–50.
10. Garg DK, Serra CA, Hoarau Y, Parida D, Bouquey M, Muller R. Analytical solution of free radical polymerization: Applications-implementing gel effect using AK model. Macromolecules 2014;47(21):7370–7.

11. Chitanov V, Petrov M. Multivariable fuzzy-neural model of polymer process. Chem Prod Process Model 2009;4(1): Article 10.
12. Rafizadeh M. Non-isothermal modelling of solution polymerization of methyl methacrylate for control purposes. Iran Polym J 2001;10(4):251–63.
13. Wan Ibrahim WH, Mujtaba IM, Alhamad BM. Optimisation of emulsion copolymerization of styrene and MMA in batch and semi-batch reactors. Chem Prod Process Model 2011;6(2): Article 2.
14. Chapra SC, Canale RP. Numerical methods for engineers, 5th ed. New York: McGraw Hill International Edition, 2006.
15. Shampine LF. Numerical solution of ordinary differential equations. New York: Chapman and Hall, 1994.
16. Shampine LF, Reichelt MW. The MATLAB ode suite. SIAM J Sci Comput 1997;18(1):1–22.
17. Soroush M, Kravaris C. Nonlinear control of a batch polymerization reactor: an experimental study. AIChE J 1992; 38(9):1429–48.
18. Baillagou PE, Soong DS. Molecular weight distribution of products of free radical nonisothermal polymerization with gel effect. Simulation for polymerization of poly(methyl methacrylate). Chem Eng Sci 1985;40(1):87–104.
19. Ray WH. On the mathematical modeling of polymerization reactors. J Macromol Sci-Rev Macromol Chem 1972;8(1):1–56.
20. Tirrell M, Galvan R, Laurence RL. Polymerization reactors. In: Carberry JJ, Verma A, editors. Chemical Reaction and Reactor Engineering. New York: Marcel Dekker, 1987.
21. Verschueren K. Handbook of environment data on organic chemicals, 2nd ed. New York: Van Nostrand Reinhold Company, 1983.
22. Smiley RA. Nitriles. Kirk-Othmer Encyclopedia of Chemical Technology. New York: John Wiley and Sons, 1981.
23. Ehrenstein GW. Polymeric materials: Structure, properties and applications. Munich: Carl Hanser Verlag GmbH & Co. KG, 2012.
24. Upreti SR, Sundaram BS, Lohi A. Optimal control determination of MMA polymerization in non-isothermal batch reactor using bifunctional initiator. Eur Polym J 2005;41(12):2893–908.
25. Vrentas JS, Duda JL, Ling HC. Self-diffusion in polymer-solvent-solvent system. J Polym Sci Polym Phys Ed 1984; 22(3):459–69.
26. Soh SK, Sundberg DC. Diffusion-controlled vinyl polymerization. IV. Comparison of theory and experiment. J Polym Sci Polym Chem Ed 1982;20(5):1345–71.
27. Tobolsky AV, Baysal B. A review of rates of initiation in vinyl polymerization: Styrene and methyl methacrylate. J Polym Sci 1953;11(5):471–86.
28. Haward RN. Occupied volume of liquids and polymers. J Macromol Sci Rev Macromol Chem 1970;4(2):191–242.
29. Liu HT, Duda JL, Vrentas JS. Influence of solvent size on the concentration dependence of polymer-solvent diffusion coefficients. Macromolecules 1980;13(6):1587–9.
30. Achilias DS, Kiparissides C. Modeling of diffusion-controlled free-radical polymerization reactions. J Appl Polym Sci 1988;35(5):1303–23.